Published in final edited form as:
*J Neurochem*. 2009 July ; 110(1): 328–342. doi:10.1111/j.1471-4159.2009.06142.x.

# Proteasome–caspase–cathepsin sequence leading to tau pathology induced by prostaglandin J2 in neuronal cells

**Lisette T. Arnaud**, **Natura Myeku**, and **Maria E. Figueiredo-Pereira**
Department of Biological Sciences, Hunter College of City University of New York, New York, New York, USA

## Abstract

Neurofibrillary tangles (NFT) are a hallmark of Alzheimer's disease. The major neurofibrillary tangle component is tau that is truncated at Asp421 (Δtau), hyperphosphorylated and aggregates into insoluble paired helical filaments. Alzheimer's disease brains also exhibit signs of inflammation manifested by activated astrocytes and microglia, which produce cytotoxic agents among them prostaglandins. We show that prostaglandin (PG) J2, an endogenous product of inflammation, induces caspase-mediated cleavage of tau, generating Δtau, an aggregation prone form known to seed tau aggregation prior to neurofibrillary tangle formation. The initial event observed upon PGJ2-treatment of human neuroblastoma SK-N-SH cells was the build-up of ubiquitinated (Ub) proteins indicating an early disruption of the ubiquitin-proteasome pathway. Apoptosis kicked in later, manifested by caspase activation and caspase-mediated cleavage of tau at Asp421 and poly (ADP-ribose) polymerase. Furthermore, cathepsin inhibition stabilized Δtau suggesting its lysosomal clearance. Upon PGJ2-treatment tau accumulated in a large perinuclear aggregate. In rat E18 cortical neuronal cultures PGJ2-treatment also generated Δtau detected in dystrophic neurites. Levels of Δtau were diminished by caspase 3 knockdown using siRNA. PGD2, the precursor of PGJ2, produced some Δtau. PGE2 generated none. Our data suggest a potential sequence of events triggered by the neurotoxic product of inflammation PGJ2 leading to tau pathology. The accumulation of Ub proteins is an early response. If cells fail to overcome the toxic effects induced by PGJ2, including accumulation of Ub proteins, apoptosis kicks in triggering caspase activation and tau cleavage, the clearance of which by cathepsins could be compromised culminating in tau pathology. Our studies are the first to provide a mechanistic link between inflammation and tau pathology.

### Keywords

caspase; cathepsin; inflammation; prostaglandin J2; proteasome; tau pathology

Inflammation is implicated in Alzheimer's disease (AD) (McGeer and McGeer 2007). A recent study with P301S mutant human tau transgenic mice established that hippocampal synaptic pathology and microgliosis could be the earliest manifestations of neurodegeneration related to tauopathies (Yoshiyama *et al*. 2007). Prominent microglial activation was shown to precede tangle formation and immunosuppression of young P301S Tg mice diminished tau pathology and increased lifespan. It was proposed that neuroinflammation is linked to early progression of tauopathies (Yoshiyama *et al*. 2007).



Address correspondence and reprint requests to Maria E. Figueiredo-Pereira, Department of Biological Sciences, Hunter College of City University of New York, 695 Park Ave., New York, NY 10065, USA. pereira@genectr.hunter.cuny.edu.

Activated microglia and astrocytes produce a variety of agents, among them prostaglandins (Minghetti 2005). The major prostaglandin produced in the CNS is prostaglandin (PG) D2 (Narumiya *et al*. 1982; Ogorochi *et al*. 1984). PGD2 levels were found to be significantly increased in the frontal cortex of AD patients compared to age matched controls (Iwamoto *et al*. 1989). PGD2 is produced by two distinct types of prostaglandin D2 synthases (PGDS): (i) the lipocalin enzyme (L-PGDS) and (ii) the hematopoietic enzyme (H-PGDS) (Urade and Eguchi 2002). In addition, PGD2 binds to G protein-coupled seven transmembrane receptors, DP1 and DP2 (Urade and Eguchi 2002), which are robustly expressed in the hippocampus and cerebral cortex (Liang *et al.* 2005). In AD patients and in Tg2576 mice, a well established AD model, the levels of H-PGDS and DP1 were found to be selectively up-regulated in microglia and astrocytes within senile plaques (Mohri *et al*. 2007). Based on these results it was suggested that PGD2 acts as a mediator of plaque associated inflammation in the AD brain (Mohri *et al*. 2007). Similarly, L-PGDS which is one of the most abundant CSF proteins produced in the brain, was localized in amyloid plaques in both AD patients and Tg2576 mice (Kanekiyo *et al*. 2007). Secreted L-PGDS in the CSF has a dual function: it increases CSF-PGD2 levels (Scher and Pillinger 2005) and also acts as a lipophilic-ligand carrier (Urade and Hayaishi 2000). L-PGDS was found to bind Aβ monomers and prevent Aβ aggregation, suggesting that L-PGDS is a major Aβ chaperone and disruption of this function could be related to the onset and progression of AD (Kanekiyo *et al*. 2007).

Prostaglandin D2 exerts both neuroprotective and neurotoxic effects through its binding to DP1 and DP2 receptors, respectively (Liang *et al*. 2005). PGD2 is very short lived and readily undergoes *in vivo* and *in vitro* non-enzymatic dehydration to generate the biologically active cyclopentenone J2 prostaglandins, which include PGJ2, Δ12-PGJ2 and 15-deoxy-Δ12,14-PGJ2 (15d-PGJ2) (Shibata *et al*. 2002).

Unlike most other classes of prostaglandins, cyclopentenone prostaglandins like PGJ2 have a cyclopentenone ring with reactive α,β-unsaturated carbonyl groups that form covalent Michael adducts with nucleophiles such as free sulfhydryls in cysteine residues of glutathione and cellular proteins (Straus and Glass 2001). Just like serine, threonine and tyrosine phosphorylation is crucial for various signal transduction pathways, it has become recently clear that a highly conserved redox reaction involving cysteine thiols in proteins provides post-translational means for regulating redox signaling (Satoh and Lipton 2007). *S*-nitrosylation of cysteine thiols by nitric oxide was first discovered, followed by the more recently revealed *S*-alkylation by electrophiles (electron deficient carbon centers). Electrophile binding by endogenous metabolites [such as PGJ2] is currently regarded as playing a crucial role in determining whether neurons will live or die (Satoh and Lipton 2007).

We focused on PGJ2 because it is potently neurotoxic and a highly reactive product of inflammation. A recent review suggested that ‘formation of cyclopentenone eicosanoids (such as PGJ2) in the brain may represent a novel pathogenic mechanism that contributes to many neurodegenerative conditions’ (Musiek *et al*. 2005). Because of their high reactivity with thiol-containing intracellular compounds like glutathione or thiol-containing proteins via Michael addition, any attempt to measure PGJ2 levels in human tissues or fluids will be highly inaccurate and will not reflect its biological activity (Uchida and Shibata 2008). Similar to PGJ2, nitric oxide has a half life of just a few seconds, and yet it is well accepted as a major signaling molecule in neurons and in the immune system (Murad 1998). The same can be said for PGJ2, i.e. that it is a major signaling molecule/oxidative stress agent.

Here we address the effect of the highly reactive lipid electrophile PGJ2 on tau cleavage in human neuroblastoma SK-N-SH cells as well as in rat primary cortical cultures. Our results demonstrate that products of inflammation such as PGJ2 have a bifunctional effect on intracellular protein turnover. They impair the ubiquitin-proteasome pathway leading to the

abnormal build-up of ubiquitinated (Ub) proteins and activate caspase-mediated proteolysis responsible for generating tau truncated at Asp421 (Δtau) that could serve as a seed for cytotoxic protein aggregation. This dual effect on intracellular protein turnover, i.e. proteasome impairment and caspase activation, set off by the product of inflammation could be a major factor in the progression of AD neurodegeneration.

## Materials and methods

### Materials

Prostaglandins J2, D2 and E2, ciglitazone and bisphenol A diglycidyl ether (BADGE) were from Cayman Chemical (Ann Arbor, MI, USA) and NAC (*N*-acetyl-cysteine) from Sigma-Aldrich, St. Louis, MO, USA. Protease inhibitors: caspase irreversible inhibitors (2 μM) for individual caspases 1 through 6, 8 through 10 and 13, the pan caspase inhibitor [Z-VAD-FMK, where Z is benzyloxycarbonyl; VAD is conventional one-letter abbreviations of amino acid; and FMK is fluoromethyl ketone], which inhibits all known caspases, and the negative control Z-FA-FMK (FA is conventional one-letter abbreviations of amino acid) were from BioVision, Mountain View, CA, USA. Pan caspase inhibitor, which inhibits all caspases and is the same as caspase inhibitor I, calpeptin (Z-Leu-Nleu-CHO), calpain inhibitor I (N-Acetyl-Leu-Leu-Nle-CHO), calpain inhibitor III (Z-Val-Phe-CHO), and Pepstatin A (Iva-Val-Val-Sta-Ala-Sta) were from Calbiochem (San Diego, CA, USA). Calpain inhibitor (Z-Leu-Leu-CHO) was from BioMol (Plymouth Meeting, PA, USA) and PSI [Z-Ile-Glu(OtBu)-Ala-Leu-CHO] from Peptides International Inc. (Louisville, KY, USA). Primary antibodies (Table. 1): Tau C3 (mouse monoclonal, tau cleaved at Asp421) 1 : 500 from Covance (Emeryville, CA, USA), Tau clone 5 (mouse monoclonal) 1 : 1000 courtesy Dr. L. Binder (Northwestern University, Chicago, IL, USA), pan tau clone 13 (mouse monoclonal) 1 : 1000 from Santa-Cruz (Santa Cruz, CA, USA), TauY9 (rabbit polyclonal) 1 : 1000 from BioMol, rabbit monoclonal anti-β tubulin (1 : 2000, clone MRB-435P) from Covance, rabbit polyclonal anti-Ub proteins (1 : 1500) from Dako Cytomation (Carpinteria, CA, USA), and anti-cleaved PARP [poly (ADP-ribose) polymerase] (1 : 1000 clone 19F4) as well as anti-caspase 3 (polyclonal, 1 : 500) from Cell Signaling Tech (Danvers, MA, USA). The respective secondary antibodies with fluorophores (1 : 50) were from Jackson ImmunoResearch Laboratories, Inc. (West Grove, PA, USA). TO-PRO-3 iodide (nuclear staining) was from Invitrogen (Carslbad, CA, USA).

### Cell cultures

SK-N-SH cells are a human neuroblastoma cell line derived from peripheral tissue (Biedler *et al*. 1978). The cells are maintained at 37 °C in minimal essential medium (MEM) with Earle's salts containing 5% normal fetal bovine serum, 2 mM L-glutamine, 1 mM sodium pyruvate, 0.4% MEM vitamins, 0.4% MEM non-essential amino acids, and 100 units/mL penicillin, 100 μg/mL streptomycin in 5% $CO_2$.

Rat E18 cortical neuronal cultures were from Neuromics (Edina, MN, USA). The cells were maintained at 37 °C in 5% $CO_2$ in neurobasal media supplemented with 2% B27 and 0.5 mM glutamine (all from Invitrogen) and half of the medium was changed every 3 days.

### Cell treatments with PGJ2

Cell cultures were treated for the indicated times with vehicle (DMSO, dimethyl sulfoxide) or with different concentrations of PGJ2, PGD2 or PGE2 in DMSO added directly to serum-containing medium. The final DMSO concentration in the medium was 0.5%. At the end of the incubation, all cultures were washed twice with phosphate buffered saline (PBS) and processed for the different assays as described below. Cell washes removed unattached cells, therefore subsequent assays were performed on adherent cells only.

### Treatment with caspase 3 siRNA

We used a highly efficient non-toxic siRNA delivery approach in which the siRNAs are linked to the vector peptide Penetratin 1 (Pen1) as described in (Davidson *et al*. 2004). Rat E18 cortical neuronal cultures were plated at a density of $9 \times 10^5$ cells in 2 mL of media per well in a six-well plate and cultured for 3 days. The cultures were then treated with 80 nM of Pen1-caspase 3-siRNA or Pen1-scrambled-siRNA for 6 h prior to treatment with vehicle (control) or PGJ2 for an additional 16 h before harvesting. The siRNAs were a gift from Dr. C. Troy (Columbia University, New York, NY, USA). The sequence for the siCasp3 was AGCCGAAACUCUUCAUCAU (GenBank accession number BC038825, initiation at base 111, target bases 569–589) and for the scramble siRNA was CCUCAUGAAAGCACUCAUU.

### Western blotting

Western blot analysis was carried out by sodium dodecyl sulfate–polyacrylamide gel electrophoresis on 8% or 10% polyacrylamide gels. After treatment cells were rinsed twice with PBS and were harvested by gently scraping into ice-cold homogenization buffer [20 mM Tris-HCl, pH 7.5, 137 mM NaCl, 1 mM EGTA, 2.5 mM $Na_4P_2O_7$,1 mM β-glycerophosphate, 50 mM NaF, 1 mM phenylmethylsulfonyl fluoride, 1% NP40 (Sigma, St Louis, MO, USA), 1mM $Na_3VO_4$, 1% Glycerol and protease inhibitor cocktail (Sigma-Aldrich)]. Samples were boiled for 5 min in Laemmli buffer and loaded onto gels (18–50 lg of protein/lane). Following electrophoresis, proteins were transferred to an Immobilon-P membrane (Millipore, Bedford, MA, USA). The membrane was probed with the respective antibodies and antigens were visualized by a standard chemiluminescent horseradish peroxidase method with the ECL reagent. As a control for protein loading the western blots were probed for actin [mouse monoclonal anti-actin (1 : 2500, clone AC-20) from Sigma-Aldrich] or β tubulin. Semi-quantitative analysis of protein detection was done by image analysis with the ImageJ program (Rasband, W.S., ImageJ, US NIH, Maryland, http://rsb.info.nih.gov/ij/, 1997–2006). Relative intensity (no units) is the ratio between the value for each protein and the value for actin.

### Cell viability

Cell survival was assessed with the 3-(4,5-dimethylthiazol-2-yl)-2,5-diphenyl tetrazolium bromide (MTT) assay as described in (Mosmann 1983). In short, cells were grown in 24-well plates under the various conditions and for different times. At the end of the incubation period, cells were subjected to the MTT assay. Water soluble yellow MTT in media is metabolized by the metabolically active cells to the water insoluble purple formazan. After 1 h incubation with MTT, the media was removed and the formazan was dissolved in 0.04 N hydrochloric acid (HCl) in isopropanol. The resulting product was quantified by spectrophotometry using a plate reader at 550 nm.

### Caspase activity assays

Caspase screening assays (for caspases 2, 3, 8 and 9) and caspase 3 assays were carried out with ApoAlert caspase kits (plates) from ClonTech (Mountain View, CA, USA). As ClonTech does not carry an assay exclusively for caspase 2, the time course for caspase 2 activation was established with a caspase 2 kit from BioVision following manufacturer's specifications.

### Immunofluorescence

After treatment cells were rinsed with PBS, fixed for 15 min at 37 °C in 2% formaldehyde in media, quenched with 50 mM $NH_4Cl$/PBS for 20 min, permeabilized with 0.1% saponin/PBS, blocked with 2% bovine serum albumin/PBS, and incubated with the antibodies listed in each figure. TO-PRO-3 iodide (Invitrogen) was used for nuclear staining. Slides were mounted with Vectashield mounting medium hard set for immunofluorescence (Vector Laboratories, Inc.,

Burlingame, CA, USA). Cell staining was visualized with a Leica TCS SP2 confocal microscope (Leica microsystems, Exton, PA, USA).

*Protein concentration* was determined with the bicinchoninic acid assay kit (Pierce, Rockford, IL, USA) or the Bradford Assay (Bio-Rad, Hercules, CA, USA).

### Statistical analysis

Statistical significance was estimated using one-way ANOVA (Tukey-Kramer multiple comparison test) or the unpaired *t*-test with the Instat 2.0, Graphpad Software (San Diego, CA, USA).

## Results

### PGJ2-treatment induces accumulation of Ub proteins, tau cleavage and apoptosis in a dose dependent manner

Tau cleavage at Asp421 is an early event in AD tangle pathology (Rissman *et al*. 2004). Furthermore, microglia activation was shown to precede tangle formation in the P301S tauopathy mouse model (Yoshiyama *et al*. 2007). We thus determined the effect of the product of inflammation PGJ2 on tau cleavage in human SK-N-SH neuroblastoma cells. We assessed tau immunoreactivity with two monoclonal antibodies: tauC3 (epitope a.a. 412–421), which is specific for tau cleaved at Asp421 (Fig. 1a), and tau13 (Fig. 1e, pan tau, epitope a.a. 2–18), which detects all tau isoforms of human origin. Tau C3 detected two major bands with an approximate molecular mass of ~ 60 kDa (⋆, unspecific) and ~44 kDa (ΔTau, tau cleaved at Asp421). while pan tau reacted with all tau isoforms as well as with Δtau. Equal protein loading was demonstrated by probing the blots with the anti-actin antibody (Fig. 1c).

It is clear that the levels of Δtau increased in a concentration-dependent manner (Fig. 1a, e and g) reaching a peak at 20 μM PGJ2 after 16 h of treatment (Fig. 1a, *boxed*). The Δtau peak coincided with a peak in apoptosis assessed by PARP cleavage (Fig. 1b and g) and with a ~53% decrease in cell survival assessed with the MTT assay (Fig. 1f). Notably, the highest levels of Ub proteins were observed in cells treated with lower concentrations of PGJ2 (10 μM) (Fig. 1d). These results indicate that the build-up of Ub proteins is more sensitive to the PGJ2 treatment than the production of Δtau.

### PGJ2-treatment induces accumulation of Ub proteins, tau cleavage and apoptosis in a time dependent manner

To establish the time-dependency of the PGJ2 effect on Δtau we incubated SK-N-SH cells with 20 μM PGJ2 for 2 h, 4 h, 8 h, 16 h and 20 h. Just like PARP cleavage (Fig. 2b and g) that is an indicator of apoptosis, Δtau was detected 16 h post PGJ2-treatment (Fig. 2a, e and g). At this time point a significant decrease (~33%) in cell survival assessed with the MTT assay was also observed (Fig. 2f). This remarkable coincidence between tau and PARP cleavages indicates that Δtau is associated with the onset of apoptosis.

The accumulation of Ub proteins was detected 2 h after the PGJ2 treatment and increased to a plateau at 4 h post-treatment (Fig. 2d and g). Clearly, the abnormal accumulation of Ub proteins precedes the onset of apoptosis and the generation of Δtau as well as cleaved PARP. These results suggest that if the cell cannot overcome the damaging effects induced by PGJ2, including the overwhelming build-up of Ub proteins, it launches caspase-mediated proteolysis.

We confirmed that the PGJ2-induced Δtau is indeed truncated tau with monoclonal and polyclonal antibodies that react with different epitopes: Tau C3 (monoclonal, epitope a.a. 412–421) from Covance, Tau clone 5 (monoclonal, epitope 210–241) courtesy from Dr. Binder,

TauY9 (polyclonal, epitope a.a. 12–27) from BioMol, and pan tau clone 13 (monoclonal, epitope a.a 2–18) from Santa-Cruz (*results not shown*).

## PGJ2-treatment activates caspases which in turn mediate tau cleavage

As Δtau coincided with the onset of apoptosis detected by PARP cleavage, we investigated if PGJ2 activates intracellular caspases. Initially, we run a caspase screening assay and established that treatment of SK-N-SH cells with 20 μM PGJ2 for 16 h, significantly ($p \leq 0.014$, *t*-test) activated all caspases tested, i.e. initiator caspases (CASP2, CASP8 and CASP9) as well as the effector caspase 3, albeit different levels of activation were observed (Fig. 3a). Not surprisingly, caspase 3 showed the greatest activation (~20-fold) upon PGJ2-treatment, as it is an effector caspase. Following 8 h of treatment with 20 μM PGJ2, caspase 3 activity was significantly higher than in control ($p < 0.001$, *asterisks*) and reached a peak (24-fold increase) by 16 h post-treatment (Fig. 3b). The peak in caspase 3 activity coincides with the peak in PARP cleavage, a known substrate for this caspase, and the Δtau peak supporting the view that tau is also a substrate for caspase 3, as addressed in the discussion. Caspase 2 activation followed a time course similar to caspase 3, albeit its peak activation only reached a 2.5-fold increase observed after 16 h of incubation with 20 μM PGJ2 (Fig. 3c).

In SK-N-SH cells tau cleavage induced by 16 h of treatment with 20 μM PGJ2 (Fig. 4a, *boxed lanes 2 and 10*) was attenuated by pre-treatment with irreversible inhibitors (2 μM) for individual caspases 1 through 6, 8 through 10 and 13 (Fig. 4a, *lanes 3–8 and 11–14*). The pan caspase inhibitor, which inhibits all known caspases, also lessened the levels of Δtau (Fig. 4a, *lane 15*). The negative control Z-FA-FMK (2 μM) did not affect full length tau (Fig. 4c) nor PGJ2-induced cleaved tau. Overall, these results clearly indicate that PGJ2-induced tau cleavage is caspase-mediated.

## Pharmacological manipulations of tau cleavage in SK-N-SH cells

There are no specific prostaglandin synthases leading to PGJ2 production and no specific PGJ2 receptors have yet been identified (Uchida and Shibata 2008). However, PGJ2 can act via the intranuclear receptor PPARγ (peroxisome proliferator-activated receptor γ) (Scher and Pillinger 2005). To test if Δtau is induced by PPARγ activation, we treated SK-N-SH cells with ciglitazone a *bone fide* PPARγ ligand. As shown in Fig. 5(a) (*lane 7*) ciglitazone did not induce tau cleavage and the PPARγ antagonist BADGE (bisphenol A diglycidyl ether) failed to prevent PGJ2-induced Δtau (Fig. 5(a), *compare boxed lane 2 with lane 3*) showing that PPARγ does not mediate this PGJ2 effect on tau.

Besides acting through receptors, PGJ2 can exert its action by covalently binding to free sulfhydryl groups on cysteines in glutathione and cellular proteins (Scher and Pillinger 2005). NAC exhibits direct and indirect antioxidant properties and binds to electrophilic groups (Dekhuijzen 2004). We thus tested if NAC prevented PGJ2-induced cleavage of tau by caspases. As seen in Fig. 5(b) (*boxed lane 6*), NAC totally prevented the formation of Δtau.

As PGJ2 is known to inhibit proteasome activity in cells (Uchida and Shibata 2008) we investigated whether a proteasome inhibitor [PSI, *N*-benzyloxycarbonyl-Ile-Glu(*O*-*t*-butyl)-Ala-leucinal] would mimic the PGJ2 effect on Δtau. As shown in Fig. 5(b) (*lanes 4 and 5*) PSI did not increase the levels of Δtau. Neither did the calpain inhibitor Z-LLCHO (Fig. 5b, *lane 3*).

We also investigated if inhibitors of other intracellular proteases prevented tau cleavage induced by PGJ2 in SK-N-SH cells. Four different calpain inhibitors (Fig. 6a) and the general cathepsin inhibitor pepstatin (Fig. 6b) failed to prevent the production of Δtau induced by PGJ2-treatment. In fact, we observed the highest levels of Δtau in cells co-treated with the pan caspase

inhibitor (20 μM) and pepstatin (100 μM) prior to PGJ2 (Fig. 6b, *boxed lane 3*). These results mimic what was observed, to a lesser extent, with PGJ2 in conjunction with 20 μM of the pan caspase inhibitor (Fig. 5a, *lane 4*). The pan caspase inhibitor Z-VAD-FMK inhibits all caspases. However, it was previously demonstrated that caspase inhibitors with FMKs also reduce the activity of lysosomal cathepsins (Schotte *et al*. 1999). These data indicate that caspase inhibitors exert a bifunctional, concentration-dependent effect on tau cleavage: low concentrations (2 μM) diminish Δtau, while high concentrations (20 μM) increase Δtau production. The latter effect may indicate that once formed, Δtau is removed by lysosomal cathepsins, which are also inhibited by the higher (20 μM) pan caspase inhibitor concentration. A similar effect was not observed on PARP, as 20 μM of the pan caspase inhibitor prevented PARP cleavage (Fig. 5a, *middle panel, lane 4*).

## PGJ2 induces the formation of a large perinuclear tau aggregate next to a nuclear indentation

The distribution of tau was altered by PGJ2 treatment. In control SK-N-SH cells tau (*green*) exhibits a uniform distribution that extends from the nuclear envelope out to the periphery of the cell (Fig. 7a, larger in d). The nucleus is stained red with a carbocyanine monomer (TO-PRO-3 iodide, Invitrogen). Upon treatment with 20 μM PGJ2 for 16 h tau immunoreactivity (Fig. 7b, larger in c) emerged as a large perinuclear aggregate (*white arrows*) next to a nuclear indentation. The large perinuclear aggregate detected in PGJ2-treated cells resembles aggresomes, first described by Kopito's group (Johnston *et al.* 1998). Aggresomes are thought to be deposition sites for proteins that escape degradation by the ubiquitin-proteasome pathway and to be co-localized with centrosome/microtubule organizing center markers such as γ-tubulin [reviewed in (Kopito 2000)].

## Tau is cleaved at Asp421 in rat E18 cortical neuronal cultures treated with PGJ2 or PGD2 but not in those treated with PGE2

We incubated rat E18 primary cortical neuronal cultures with 20 μM PGJ2 or 20 μM PGD2 or 80 μM PGE2 for 16 h. Physiological concentrations of prostaglandins in body fluids are found to be in the pico-nanomolar range (Fukushima 1990). However, their levels rise considerably under pathological conditions such as hyperthermia, infection, and inflammation, reaching the micromolar range at the site of damage (Herschman *et al*. 1997). The prostaglandin concentrations used herein were based on our previous studies with rat primary neuronal cultures, which compared the cytotoxicity of PGD2, PGE2 and PGJ2 within a range of concentrations used in most publications (Li *et al*. 2004). PGJ2 was the most toxic (20 μM, 50% cell death) followed by PGD2 (20 μM, 40% cell death) and PGE2 (80 lM, 35% cell death, reaching a plateau).

As shown in Fig. 8(a) (*lanes 3 and 6*, designated C and E2) the TauC3 antibody did not react with any major tau bands in control cultures or cultures treated with 80 μM PGE2, respectively. In cells treated with 20 μM PGJ2 (*boxed lane 4*)or 20 μM PGD2 (*lane 5*) TauC3 immunoreactivity detected truncated tau (Δtau) with a molecular mass similar to Δtau identified in human SK-N-SH cells treated with PGJ2 (*lane 2*). The pan tau C5 antibody (Fig. 8b) detected full length tau in rat neuronal control cultures (*lane 3*) and full length as well as Δtau in PGJ2-treated cultures (*boxed lane 4*. The pan tau antibody (clone 13) detected full length tau in control SK-N-SH cells (*lane 1*) and full length as well as Δtau in PGJ2-treated cells (*lane 2*). Stripping and reprobing the blot with the anti-ubiquitin conjugates antibody (Fig. 8c) demonstrated that, just like with the human SK-N-SH cells (*lane 2*), PGJ2 (*boxed lane 4*) and PGD2 (*lane 5*) increased the levels of Ub proteins in the primary neuronal cultures, while PGE2 (*lane 6*) did not. The blots were probed with anti-actin as protein loading control (Fig. 8d).

To further establish that caspase 3 mediates tau cleavage at Asp421, we induced caspase 3 knock down by siRNA prior to treatment with vehicle (control) or PGJ2. Caspase 3 siRNA

(casp3 siRNA) clearly decreased the levels of procaspase 3 in both control and PGJ2-treated cells (Fig. 9a, *compare lanes 3 and 4 with 1 and 2*). In addition, casp3 siRNA caused a decline in the levels of Δtau as well as cleaved caspase 3 (ΔCasp3) as shown in Fig. 9(b) and (c), respectively. A scrambled siRNA failed to lower the levels of pro-caspase 3 and Δtau (Fig. 9g and h) as well as ΔCasp3 (*not shown*). These data provide strong support for a caspase 3 role in tau cleavage induced by PGJ2-treatment.

Upon immunofluorescent analysis with the TauC3 (*green*) and β tubulin (*red*) antibodies, dystrophic-like neurites were observed in the cortical neuronal cultures treated with PGJ2 (Fig. 10, *bottom panels*). Sites of neuritic dystrophy are indicated by bulb-like accumulations (*white arrows*) of tau (*green*) and β tubulin (*red*) in the PGJ2-treated neurons. Control cultures did not exhibit any immunofluorescence with the TauC3 antibody (*not shown*). This is not surprising, as shown in Fig. 8(a) (*lane 3*), no immunoreactivity was detected by western blot analysis with TauC3 under control conditions. However, immunofluorescence of control cortical cultures with the TauC5 (*green*) and β tubulin (*red*) antibodies showed no dystrophic neurites (Fig. 10, *top panels*).

## Discussion

### PGJ2 modulates tau cleavage (Asp421) through caspase mediated proteolysis

Our study provides the first evidence that a product of inflammation, PGJ2, modulates tau cleavage at Asp421 through caspase-mediated proteolysis in neuronal cells. This is important in view of the fact that studies from other groups indicate that caspase-cleavage of tau at Asp421 is an early event in AD tangle pathology (Rissman *et al*. 2004; Guillozet-Bongaarts *et al*. 2005). We also demonstrate for the first time that PGJ2-treatment induces tau cleavage at Asp421 (Δtau) which coincides with the onset of apoptosis indicated by caspase activation as well as by the concurrence of tau and PARP cleavage. Only caspase inhibitors attenuated Δtau levels induced by PGJ2-treatment. Caspase 3 knock down by siRNA also decreases Δtau levels in PGJ2-treated cells. Neither calpain nor cathepsin inhibitors diminished Δtau levels. Our data also indicate that Δtau must be cleared by lysosomal proteases, as cathepsin inhibition by pepstatin or by high concentrations (20 μM) of caspase inhibitors that also affect cathepsins (Schotte *et al*. 1999), caused an increase in Δtau levels induced by PGJ2-treatment. Together these studies provide a mechanistic link between a product of inflammation and tau pathology.

### Tau cleavage induced by PGJ2-treatment is PPARγ-independent but oxidation-dependent

Our data show that tau cleavage induced by PGJ2-treatment is PPARγ-independent. A PPARγ activator (ciglitazone) failed to mimic the effect of PGJ2-treatment on tau and a PPARγ-antagonist (BADGE) failed to prevent tau cleavage in cells treated with PGJ2. This is not surprising, as PPARγ-agonists have been linked to neuroprotection rather than neurotoxicity (Aoun *et al*. 2003). In fact PPARγ agonists are being considered as AD therapeutic agents because they modulate inflammatory responses (Jiang *et al*. 2008). However, the protective effect of PPARγ-agonists seems to be mediated by an anti-oxidant effect (Aoun *et al*. 2003). The finding that the anti-oxidant NAC prevents tau cleavage induced by PGJ2-treatment as well as other PGJ2-dependent toxic effects (Uchida and Shibata 2008), supports the view that PGJ2 neurotoxicity is indeed mediated by its pro-oxidant nature.

### Potential link between proteasome impairment and caspase-mediated tau cleavage induced by PGJ2

Alzheimer's disease and many other neurodegenerative disorders, such as Parkinson's disease and amyotrophic lateral sclerosis, share an intriguing morphological feature that is the intracellular deposition of aggregated and Ub proteins in neurons of the affected CNS areas [reviewed in (Alves-Rodrigues *et al*. 1998)]. The relationship between the accumulation of Ub

proteins, which is a general phenomenon in these disorders, and more disease-specific pathology such as neurofibrillary tangles in AD remains to be elucidated.

Our studies suggest that the abnormal build-up of Ub proteins is an early event in the cytotoxic response to PGJ2. Prostaglandins of the J2 series inhibit proteasome activity (Shibata *et al*. 2003; Ishii and Uchida 2004; Ishii *et al*. 2005; Ogburn and Figueiredo-Pereira 2006; Wang *et al*. 2006) and deubiquitination (Mullally *et al*. 2001; Ishii and Uchida 2004; Li *et al*. 2004). By covalently binding to cysteine thiol groups in proteins through Michael addition, J2 prostaglandins also provoke changes in protein tertiary structure (Ishii and Uchida 2004) that could impede protein degradation and lead to protein accumulation. All of these effects on the ubiquitin-proteasome pathway and its substrates induced by PGJ2 will have a devastating impact on proteasome activity bringing about the build-up of pro-apoptotic and detrimental proteins, such as p53 and Ub proteins (Uchida and Shibata 2008).

Our finding that the build-up of Ub proteins upon PGJ2-treatment seems to precede the onset of apoptosis supports the notion that cells launch the pro-death pathway if they fail to recover from the damaging effects of PGJ2, including generation of overwhelming levels of Ub proteins. Once apoptosis is activated caspase-mediated proteolysis kicks in leading to the generation of truncated tau. This sequence of events induced by the product of inflammation PGJ2 supports a potential cross-talk between pro-toxic effects, such as oxidative stress and proteasome impairment, and caspase activation that culminates in neurodegeneration. Notably, PGD2 that is the most abundant prostaglandin in the CNS, was not as effective as PGJ2 in inducing the production of Δtau. It is likely that the PGD2 effect on tau cleavage is dependent on its spontaneous conversion to its metabolite PGJ2. PGE2, another major CNS prostaglandin, failed to induce tau truncation.

During apoptosis, dramatic nuclear and cytoplasmic morphological changes facilitate the breakdown of cells into apoptotic bodies to ensure maintenance of intact cellular membranes and efficient removal by phagocytes or neighboring cells (Marceau *et al*. 2007). To accomplish this, caspases are known to cleave several cytoskeletal proteins, such as actin, tubulin, fodrin and vimentin [reviewed in (Luthi and Martin 2007)]. It is possible that being a cytoskeletal protein as well, tau is just another of the caspase substrates that are cleaved in the apoptotic pathway to ensure cell collapse. However, because of its propensity to aggregate, truncated tau seems to facilitate protein aggregation. Interestingly, Δtau seems more prone to adopt the MC1 conformation than full length tau. The MC1 conformation is the result of the folding of the N-terminal segment of tau which interacts with the microtubule binding region (Gamblin *et al*. 2003). MC1 is a distinct conformation of tau in AD, that precedes paired helical filaments formation and is detected in Braak stage I and II (Weaver *et al*. 2000).

*In vitro* cleavage assays of full length tau in the presence of various caspases show that tau is more susceptible to the protease activity of executioner caspases (−3, −7) than initiator caspases (−1, −4, −5, −8, −10) (Gamblin *et al*. 2003). The resulting products include a C-terminal 45.9 kDa fragment and a small 2 kDa fragment. Our studies show (Fig. 4) considerable variation in the activity remaining following specific caspase inhibitions. This may be because of the inherent non-specificity of the supposedly specific caspase inhibitors currently available or an indication that caspases 2–4 are the most important with respect to the formation of cleaved tau. The reduced effect of the pan caspase inhibitor on tau cleavage could be caused by it being a more effective cathepsin inhibitor than the other caspase inhibitors tested. These possibilities will be addressed in future studies.

## Perinuclear tau aggregates and dystrophic neurites

Full-length tau is a highly soluble protein, yet in AD it appears as abnormal aggregates. Previous studies propose that truncated tau induces the aggregation of full-length tau and that

tau aggregates are toxic to cells (Gamblin *et al*. 2003; Cho and Johnson 2004; Rissman *et al*. 2004; Wang *et al*. 2007). Therefore, Δtau may serve as a seed for cytotoxic protein aggregation. In our previous studies we demonstrated that PGJ2 induces the collapse of the cytoskeleton/endoplasmic reticulum (Ogburn and Figueiredo-Pereira 2006). The PGJ2-dependent cytoskeletal rearrangement paralleled the development of a large aggregate at the microtubule organizing center co-localized with γ-tubulin and also containing Ub proteins. We now demonstrate that this perinuclear aggregate that resembles an aggresome (Johnston *et al*. 1998) is also enriched in tau. These data suggest that tau is driven to the perinuclear aggregate by the microtubule collapse.

We also established that PGJ2 caused neurite dystrophy in rat E18 primary cortical neurons indicating that neuritic pathology is not always linked to amyloid plaques. Notably, immunoelectron microscopy studies with AD brains demonstrated the presence of cathepsin-containing autophagolysosomes in dystrophic neurites (Nixon *et al*. 2005). These results together with our data showing that cathepsin inhibition leads to an increase in Δtau levels, suggest that autophagy may be involved in Δtau clearance. In conclusion, it is clear that PGJ2 is not the only cytotoxic agent produced by activated glia (microglia and astrocytes) as a result of the chronic inflammatory process. Other factors, such as nitric oxide, interleukin 1β, interleukin 6, tumor necrosis factor α and reactive oxygen species (e.g. super-oxide anion) are also produced under conditions of inflammation. All of these cytotoxic agents must work in concert to induce synergistic neurotoxicity leading to neurodegeneration (Liu *et al*. 2003; Klegeris *et al*. 2007). Based on the data obtained with PGJ2 we propose a model in which any stimulus (physical, chemical or infectious) that induces inflammation in a particular brain area, activates microglia and astrocytes. The activated glia release toxic products (such as PGJ2) onto neighboring neurons causing impairment of the ubiquitin-proteasome pathway and/or overwhelming proteasome activity leading to the accumulation of Ub proteins. If removal of the Ub proteins as well as reversal of other damaging effects induced by the neurotoxic products of inflammation fails to occur, apoptosis is triggered. During apoptosis, caspase-mediated proteolysis cleaves cytoskeletal proteins including tau, which promotes cytotoxic protein aggregation and in conjunction with caspase activation promotes cell death. A potential link between accumulation of Ub protein, proteasome impairment and caspase activation triggered by products of inflammation could explain many pathological features of AD including tau pathology.

## Acknowledgments

We thank Dr. L. Binder (Northwestern University, Chicago) for the Tau clone 5 antibody and Dr. C. Troy (Columbia University, New York) for the caspase 3 and scrambled siRNAs. This work was supported by NIH: NINDS-NS41073 (SNRP), M.E.F.-P head of sub-project and NCRR-RR03037 (infrastructure) to Hunter College, City University of New York. There are no conflicts of interest.

## Abbreviations used

| | |
|---|---|
| Δtau | tau truncated at Asp421 |
| AD | Alzheimer's disease |
| BADGE | bisphenol A diglycidyl ether |
| DMSO | dimethyl sulfoxide |
| FMK | fluoromethyl ketone |
| MEM | minimal essential medium |
| MTT | 3-(4,5-dimethylthiazol-2-yl)-2,5-diphenyl tetrazolium bromide |

| | |
|---|---|
| NAC | *N*-acetyl-cysteine |
| PARP | poly (ADP-ribose) polymerase |
| PBS | phosphate buffered saline |
| Pen1 | vector peptide Penetratin 1 |
| PG | pros-taglandin |
| PGDS | prostaglandin D2 synthases |
| PPARγ | peroxisome proliferator-activated receptor γ |
| PSI | *N*-benzyloxycarbonyl-Ile-Glu(*O*-*t*-butyl)-Ala-leucinal |
| Ub | ubiquitinated |
| Z | benzyloxycarbonyl |

## References


Alves-Rodrigues A, Gregori L, Figueiredo-Pereira ME. Ubiquitin, cellular inclusions and their role in neurodegeneration. Trends Neurosci 1998;21:516–520. [PubMed: 9881849]

Aoun P, Simpkins JW, Agarwal N. Role of PPAR-gamma ligands in neuroprotection against glutamate-induced cytotoxicity in retinal ganglion cells. Invest. Ophthalmol. Vis. Sci 2003;44:2999–3004. [PubMed: 12824244]

Biedler JL, Roffler-Tarlov S, Schachner M, Freedman LS. Multiple neurotransmitter synthesis by human neuroblastoma cell lines and clones. Cancer Res 1978;38:3751–3757. [PubMed: 29704]

Cho JH, Johnson GV. Glycogen synthase kinase 3 beta induces caspase-cleaved tau aggregation in situ. J. Biol. Chem 2004;279:54716–54723. [PubMed: 15494420]

Davidson TJ, Harel S, Arboleda VA, Prunell GF, Shelanski ML, Greene LA, Troy CM. Highly efficient small interfering RNA delivery to primary mammalian neurons induces MicroRNA-like effects before mRNA degradation. J. Neurosci 2004;24:10040–10046. [PubMed: 15537872]

Dekhuijzen PN. Antioxidant properties of N-acetylcysteine: their relevance in relation to chronic obstructive pulmonary disease. Eur. Respir. J 2004;23:629–636. [PubMed: 15083766]

Fukushima M. Prostaglandin J2–anti-tumour and anti-viral activities and the mechanisms involved. Eicosanoids 1990;3:189–199. [PubMed: 2073399]

Gamblin TC, Chen F, Zambrano A, et al. Caspase cleavage of tau: linking amyloid and neurofibrillary tangles in Alzheimer's disease. Proc. Natl Acad. Sci. USA 2003;100:10032–10037. [PubMed: 12888622]

Guillozet-Bongaarts AL, Garcia-Sierra F, Reynolds MR, Horowitz PM, Fu Y, Wang T, Cahill ME, Bigio EH, Berry RW, Binder LI. Tau truncation during neurofibrillary tangle evolution in Alzheimer's disease. Neurobiol. Aging 2005;26:1015–1022. [PubMed: 15748781]

Herschman HR, Reddy ST, Xie W. Function and regulation of prostaglandin synthase-2. Adv. Exp. Med. Biol 1997;407:61–66. [PubMed: 9321932]

Ishii T, Uchida K. Induction of reversible cysteine-targeted protein oxidation by an endogenous electrophile 15-deoxy-delta12,14-prostaglandin J2. Chem. Res. Toxicol 2004;17:1313–1322. [PubMed: 15487891]

Ishii T, Sakurai T, Usami H, Uchida K. Oxidative modification of proteasome: identification of an oxidation-sensitive subunit in 26 s proteasome. Biochemistry 2005;44:13893–13901. [PubMed: 16229478]

Iwamoto N, Kobayashi K, Kosaka K. The formation of prostaglandins in the postmortem cerebral cortex of Alzheimer-type dementia patients. J. Neurol 1989;236:80–84. [PubMed: 2709057]

Jiang Q, Heneka M, Landreth GE. The role of peroxisome proliferator-activated receptor-gamma (PPARgamma) in Alzheimer's disease: therapeutic implications. CNS Drugs 2008;22:1–14. [PubMed: 18072811]

Johnston JA, Ward CL, Kopito RR. Aggresomes: a cellular response to misfolded proteins. J. Cell Biol 1998;143:1883–1898. [PubMed: 9864362]

Kanekiyo T, Ban T, Aritake K, et al. Lipocalin-type prostaglandin D synthase/beta-trace is a major amyloid beta-chaperone in human cerebrospinal fluid. Proc. Natl Acad. Sci. USA 2007;104:6412–6417. [PubMed: 17404210]

Klegeris A, McGeer EG, McGeer PL. Therapeutic approaches to inflammation in neurodegenerative disease. Curr. Opin. Neurol 2007;20:351–357. [PubMed: 17495632]

Kopito RR. Aggresomes, inclusion bodies and protein aggregation. Trends Cell Biol 2000;10:524–530. [PubMed: 11121744]

Li Z, Melandri F, Berdo I, Jansen M, Hunter L, Wright S, Valbrun D, Figueiredo-Pereira ME. delta12-Prostaglandin J2 inhibits the ubiquitin hydrolase UCH-L1 and elicits ubiquitin–protein aggregation without proteasome inhibition. Biochem. Biophys. Res. Commun 2004;319:1171–1180. [PubMed: 15194490]

Liang X, Wu L, Hand T, Andreasson K. Prostaglandin D2 mediates neuronal protection via the DP1 receptor. J. Neurochem 2005;92:477–486. [PubMed: 15659218]

Liu B, Gao HM, Hong JS. Parkinson's disease and exposure to infectious agents and pesticides and the occurrence of brain injuries: role of neuroinflammation. Environ. Health Perspect 2003;111:1065–1073. [PubMed: 12826478]

Luthi AU, Martin SJ. The CASBAH: a searchable database of caspase substrates. Cell Death Differ 2007;14:641–650. [PubMed: 17273173]

Marceau N, Schutte B, Gilbert S, Loranger A, Henfling ME, Broers JL, Mathew J, Ramaekers FC. Dual roles of intermediate filaments in apoptosis. Exp. Cell Res 2007;313:2265–2281. [PubMed: 17498695]

McGeer PL, McGeer EG. NSAIDs and Alzheimer disease: epidemiological, animal model and clinical studies. Neurobiol. Aging 2007;28:639–647. [PubMed: 16697488]

Minghetti L. Role of inflammation in neurodegenerative diseases. Curr. Opin. Neurol 2005;18:315–321. [PubMed: 15891419]

Mohri I, Kadoyama K, Kanekiyo T, et al. Hematopoietic prostaglandin D synthase and DP1 receptor are selectively upregulated in microglia and astrocytes within senile plaques from human patients and in a mouse model of Alzheimer disease. J. Neuropathol. Exp. Neurol 2007;66:469–480. [PubMed: 17549007]

Mosmann T. Rapid colorimetric assay for cellular growth and survival: application to proliferation and cytotoxicity assays. J. Immunol. Methods 1983;65:55–63. [PubMed: 6606682]

Mullally JE, Moos PJ, Edes K, Fitzpatrick FA. Cyclopentenone prostaglandins of the J series inhibit the ubiquitin isopeptidase activity of the proteasome pathway. J. Biol. Chem 2001;276:30366–30373. [PubMed: 11390388]

Murad F. Nitric oxide signaling: would you believe that a simple free radical could be a second messenger, autacoid, paracrine substance, neurotransmitter, and hormone? Recent Prog. Horm. Res 1998;53:43–59. [PubMed: 9769702]

Musiek ES, Milne GL, McLaughlin B, Morrow JD. Cyclopentenone eicosanoids as mediators of neurodegeneration: a pathogenic mechanism of oxidative stress-mediated and cyclooxygenase-mediated neurotoxicity. Brain Pathol 2005;15:149–158. [PubMed: 15912888]

Narumiya S, Ogorochi T, Nakao K, Hayaishi O. Prostaglandin D2 in rat brain, spinal cord and pituitary: basal level and regional distribution. Life Sci 1982;31:2093–2103. [PubMed: 6960222]

Nixon RA, Wegiel J, Kumar A, Yu WH, Peterhoff C, Cataldo A, Cuervo AM. Extensive involvement of autophagy in Alzheimer disease: an immuno-electron microscopy study. J. Neuropathol. Exp. Neurol 2005;64:113–122. [PubMed: 15751225]

Ogburn KD, Figueiredo-Pereira ME. Cytoskeleton/endoplasmic reticulum collapse induced by prostaglandin J2 parallels centrosomal deposition of ubiquitinated protein aggregates. J. Biol. Chem 2006;281:23274–23284. [PubMed: 16774923]

Ogorochi T, Narumiya S, Mizuno N, Yamashita K, Miyazaki H, Hayaishi O. Regional distribution of prostaglandins D2, E2, and F2 alpha and related enzymes in postmortem human brain. J. Neurochem 1984;43:71–82. [PubMed: 6427411]

Rissman RA, Poon WW, Blurton-Jones M, Oddo S, Torp R, Vitek MP, LaFerla FM, Rohn TT, Cotman CW. Caspase-cleavage of tau is an early event in Alzheimer disease tangle pathology. J. Clin. Invest 2004;114:121–130. [PubMed: 15232619]

Satoh T, Lipton SA. Redox regulation of neuronal survival mediated by electrophilic compounds. Trends Neurosci 2007;30:37–45. [PubMed: 17137643]

Scher JU, Pillinger MH. 15d-PGJ2: the anti-inflammatory prostaglandin? Clin. Immunol 2005;114:100–109. [PubMed: 15639643]

Schotte P, Declercq W, Van HS, Vandenabeele P, Beyaert R. Non-specific effects of methyl ketone peptide inhibitors of caspases. FEBS Lett 1999;442:117–121. [PubMed: 9923616]

Shibata T, Kondo M, Osawa T, Shibata N, Kobayashi M, Uchida K. 15-Deoxy-delta 12,14-prostaglandin J2. A prostaglandin D2 metabolite generated during inflammatory processes. J. Biol. Chem 2002;277:10459–10466. [PubMed: 11786541]

Shibata T, Yamada T, Kondo M, Tanahashi N, Tanaka K, Nakamura H, Masutani H, Yodoi J, Uchida K. An endogenous electrophile that modulates the regulatory mechanism of protein turnover: inhibitory effects of 15-deoxy-delta(12,14)-prostaglandin J2 on proteasome. Biochemistry 2003;42:13960–13968. [PubMed: 14636064]

Straus DS, Glass CK. Cyclopentenone prostaglandins: new insights on biological activities and cellular targets. Med. Res. Rev 2001;21:185–210. [PubMed: 11301410]

Uchida K, Shibata T. 15-Deoxy-delta(12,14)-prostaglandin J2: an electrophilic trigger of cellular responses. Chem. Res. Toxicol 2008;21(1):138–144. [PubMed: 18052108]

Urade Y, Eguchi N. Lipocalin-type and hematopoietic prostaglandin D synthases as a novel example of functional convergence. Prostaglandins Other Lipid Mediat 2002;68–69:375–382.

Urade Y, Hayaishi O. Prostaglandin D synthase: structure and function. Vitam. Horm 2000;58:89–120. [PubMed: 10668396]

Wang Z, Aris VM, Ogburn KD, Soteropoulos P, Figueiredo-Pereira ME. Prostaglandin J2 alters pro-survival and pro-death gene expression patterns and 26 S proteasome assembly in human neuroblastoma cells. J. Biol. Chem 2006;281:21377–21386. [PubMed: 16737963]

Wang YP, Biernat J, Pickhardt M, Mandelkow E, Mandelkow EM. Stepwise proteolysis liberates tau fragments that nucleate the Alzheimer-like aggregation of full-length tau in a neuronal cell model. Proc. Natl Acad. Sci. USA 2007;104:10252–10257. [PubMed: 17535890]

Weaver CL, Espinoza M, Kress Y, Davies P. Conformational change as one of the earliest alterations of tau in Alzheimer's disease. Neurobiol. Aging 2000;21:719–727. [PubMed: 11016541]

Yoshiyama Y, Higuchi M, Zhang B, Huang SM, Iwata N, Saido TC, Maeda J, Suhara T, Trojanowski JQ, Lee VM. Synapse loss and microglial activation precede tangles in a P301S tauopathy mouse model. Neuron 2007;53:337–351. [PubMed: 17270732]

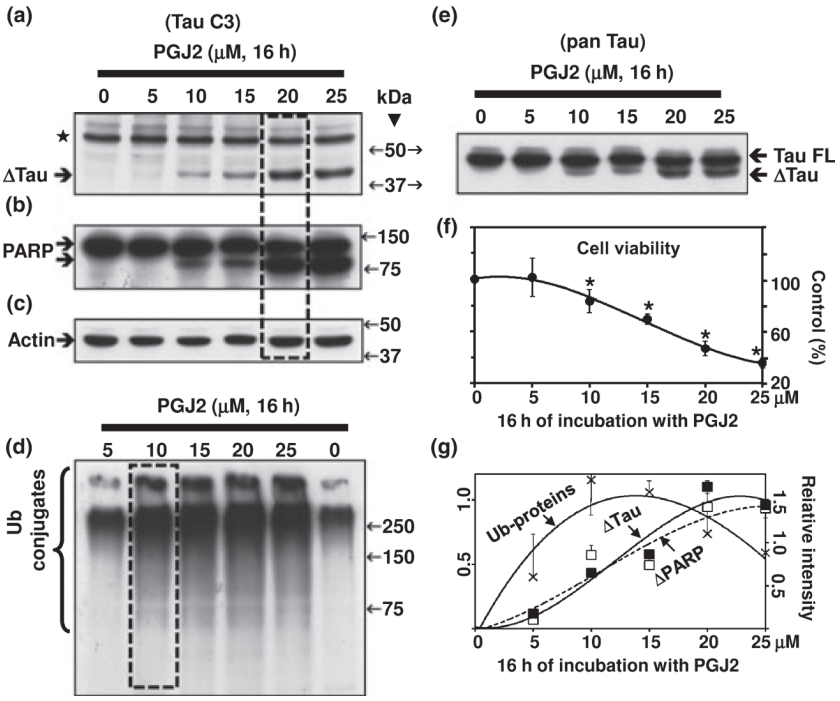


**Fig. 1.**

PGJ2-treatment induces accumulation of ubiquitinated proteins, tau cleavage and apoptosis in a dose-dependent manner. (a) and (e) Western blot analyses (10% gels) to detect tau in total extracts of human SK-N-SH neuroblastoma cells (30 lg of protein/lane) treated with PGJ2 for 16 h. In (a) the blot was probed with the TauC3 antibody (tau cleaved at Asp421, epitope a.a. 412–421). In (e) the blot was probed with the pan tau (clone 13, epitope a.a. 2–18) antibody which reacts with all tau isoforms. Equal protein loading was demonstrated by probing the immunoblots with the anti-actin antibody (c). (b) Blots were stripped and reprobed with the anti-PARP antibody, which detects cleaved PARP, an apoptosis marker. (d) Blots were stripped and reprobed again with the anti-ubiquitinated (Ub) proteins antibody. (f) Cell viability was assessed with the MTT assay. Data represent the mean ± SEM from at least three determinations. The viability for each condition was compared to the viability of cells treated with vehicle only (control, 100%). The asterisk (*) identifies the values that are significantly different ($p < 0.001$) from the control. (g) The levels of Ub-proteins (crosses), Δtau (*solid squares*) and cleaved PARP (*open squares*) were semi-quantified by densitometry. Data represent the relative intensity for Δtau and cleaved PARP (*right scale*) or Ub-proteins (*left scale*) for each PGJ2-concentration. The values obtained under control (no PGJ2) conditions were subtracted from each sample. Values represent means and SD from duplicate experiments. Molecular mass markers in kDa are shown in the middle. Boxes highlight the peaks in Δtau levels (a) and Ub-proteins (d). ΔTAU, tau cleaved at Asp421; TAU FL, full length TAU; ⋆, unspecific band.

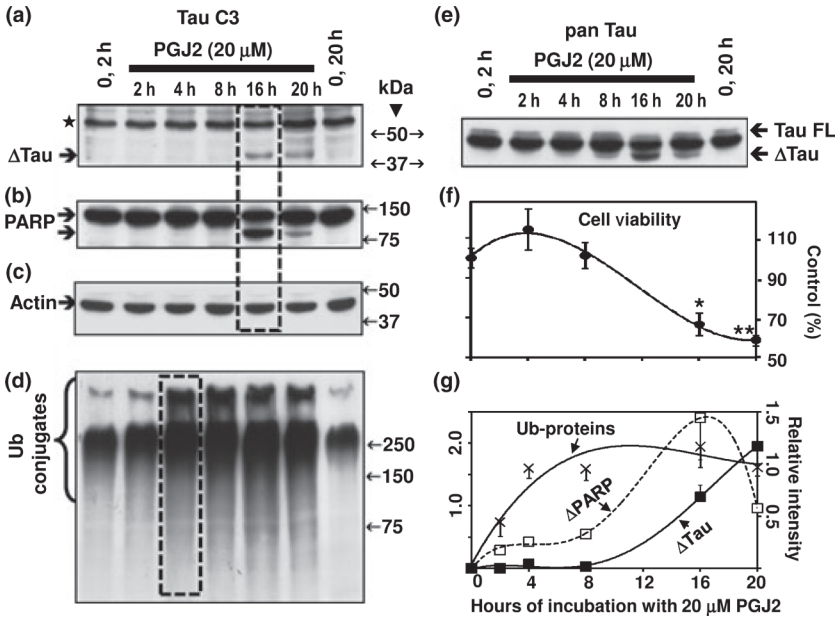


**Fig. 2.**

PGJ2-treatment induces accumulation of ubiquitinated proteins, tau cleavage and apoptosis in a time-dependent manner. (a) and (e) Western blot analyses (10% gels) to detect tau in total extracts of human SK-N-SH neuroblastoma cells (30 μg of protein/lane) treated with 20 μM PGJ2 for different times (2 h, 4 h, 8 h, 16 h, and 20 h). In (a) the blot was probed with the TauC3 antibody (tau cleaved at Asp421, epitope a.a. 412–421). In (e) the blot was probed with the pan tau (clone 13, epitope a.a. 2–18) antibody which reacts with all tau isoforms. Equal protein loading was demonstrated by probing the immunoblots with the anti-actin antibody (c). (b) Blots were stripped and reprobed with the anti-PARP antibody, which detects cleaved PARP, an apoptosis marker. (d) Blots were stripped and reprobed again with the anti-ubiquitinated (Ub) proteins antibody. (f) Cell viability was assessed with the MTT assay. Data represent the mean ± SEM from at least three determinations. The viability of cells treated with 20 μM PGJ2 for each time point was compared to the viability of cells treated with vehicle only for 20 h (control, 100%). The asterisks identify the values that are significantly different (*$p < 0.05$; **$p < 0.01$) from the control. (g) The levels of Ub-proteins (*crosses*), Δtau (*solid squares*) and cleaved PARP (*open squares*) were semi-quantified by densitometry. Data represent the relative intensity for Δtau and cleaved PARP (*left scale*) or ub-proteins (*right scale*) for each time point. The values obtained under control (no PGJ2) conditions were subtracted from each sample. Values represent means and SD from duplicate experiments. Molecular mass markers in kDa are shown on the middle. Boxes highlight the peaks in Δtau (a), cleaved PARP (b) and Ub-protein (d) levels. TAU, tau cleaved at Asp421; TAU FL, full length TAU; ⋆, unspecific band.

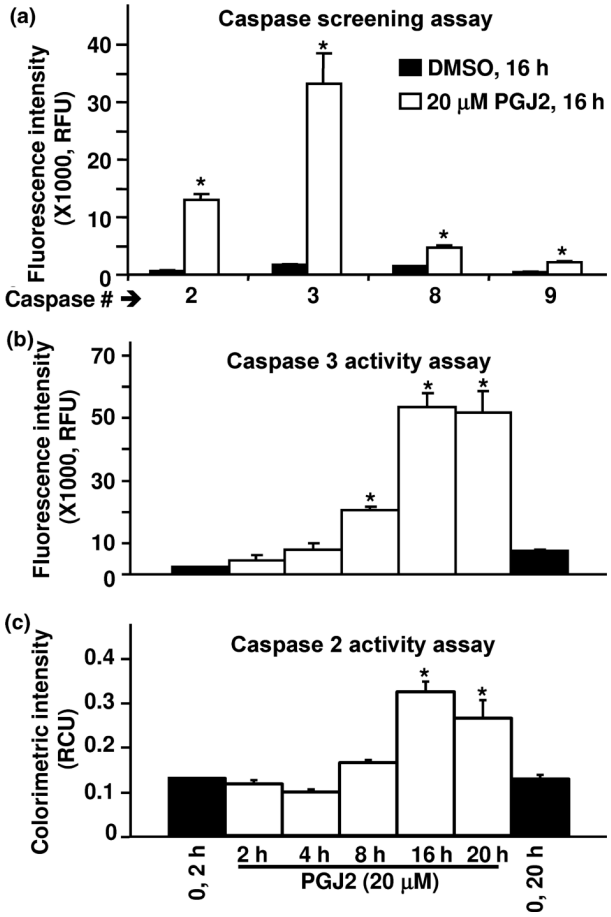


**Fig. 3.**

PGJ2-treatment increases caspase activity. (a) The activities of caspases 2, 3, 8 and 9 were determined in SK-N-SH cells treated with DMSO (vehicle, black bars) or treated with 20 μM PGJ2 (white bars) for 16 h. Relative caspase activities (RFU = relative fluorescent units) normalized for protein (200 lg/assay) are shown. Results from two determinations are presented (mean ± SD). The asterisk (*) identifies the values that are significantly different ($p \leq 0.014$, *t*-test) from the controls. (b) Caspase 3 and (c) Caspase 2 activities were determined in SK-N-SH cells treated with DMSO (vehicle, 2 h and 20 h, *black bars*) or treated with 20 μM PGJ2 (*white bars*) for 2 h, 4 h, 8 h, 16 h, and 20 h. Relative caspase activities (RFU or RCU = relative fluorescent or colorimetric units, respectively) normalized for protein (200 μg/assay) are shown. Results from at least two determinations are presented [mean ± SEM (b) and SD (c)]. The *asterisk* (*) identifies the values that are significantly different (at least $p < 0.01$, ANOVA, Tukey-Kramer multiple comparison test) from the control.

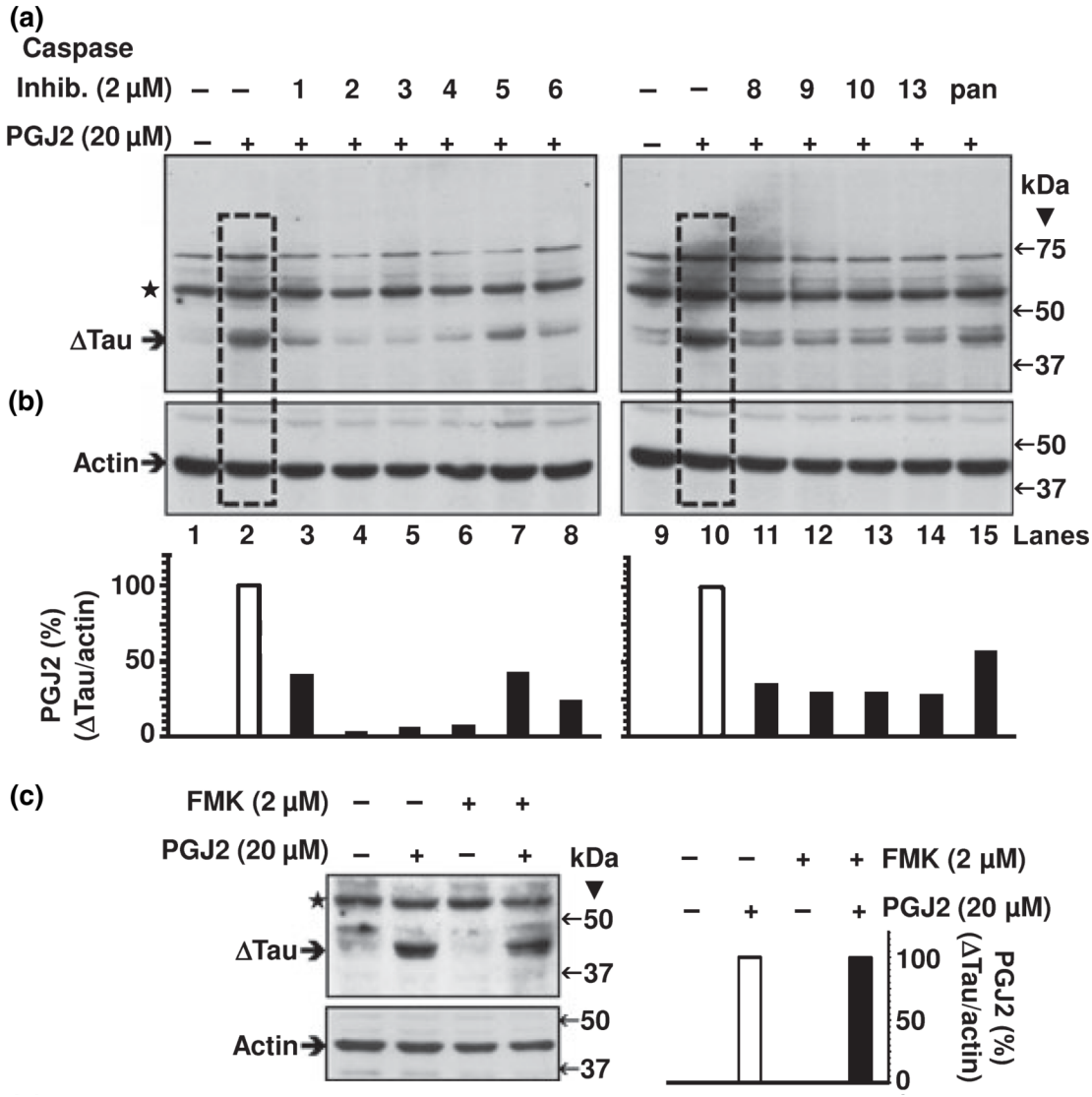


**Fig. 4.**

Individual caspase inhibitors (2 μM) attenuate the PGJ2-dependent increase in Δtau levels. ΔTau levels in total extracts of human SK-N-SH neuroblastoma cells (50 μg of protein/lane) were assessed by western blot analysis with the Tau C3 antibody (tau cleaved at Asp421, epitope a.a. 412–421). Cells were treated for 16 h with DMSO (vehicle, control, *lanes 1 and 9*) or with 20 μM PGJ2 alone (*lanes 2 and 10, boxed*) or with 20 μM PGJ2 after a 40-min pre-incubation with 2 μM of individual caspase inhibitors (1 through 6, lanes 3–8; 8 through 10, lanes 11–13, and 13, lane 14) or the pan caspase inhibitor (Z-VAD-FMK, lane 15). (c) As an FMK negative control, cells were separately incubated with Z-FA-FMK in the absence and presence of PGJ2. The levels of Δtau and actin in (a) through (c) were semi-quantified by densitometry. The data represent the ratio of Δtau/actin for all conditions compared to the PGJ2-treatment by itself (*white bars*), which was considered to be 100%. Values are from a representative experiment. Similar results were obtained in duplicate experiments. Molecular mass markers in kDa are shown on the right. ΔTau, tau cleaved at Asp421; ⋆, unspecific band.

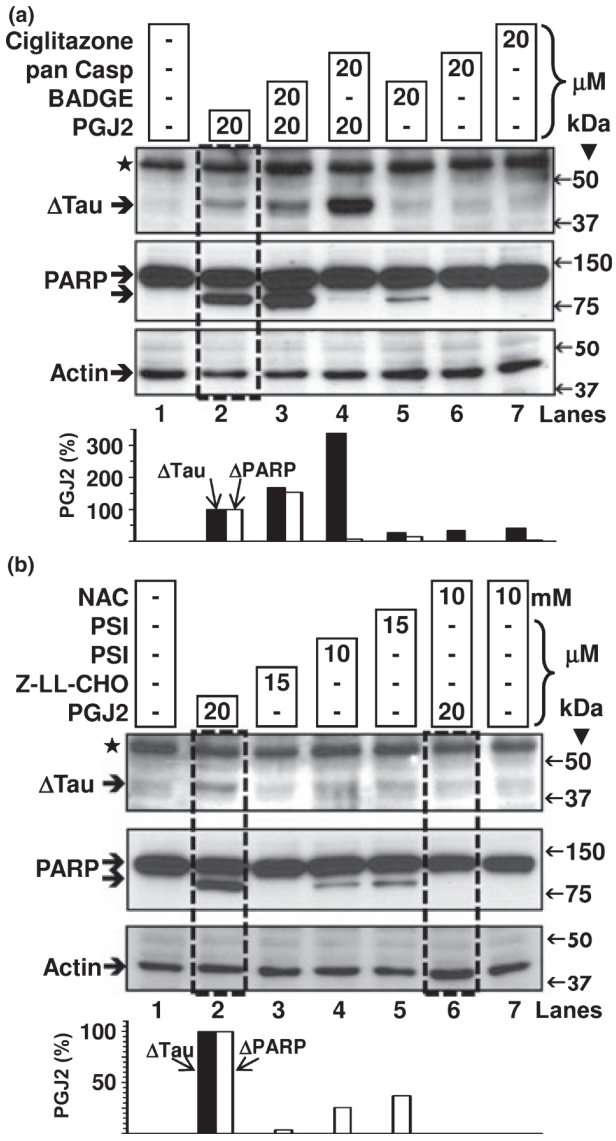


**Fig. 5.**

Pharmacological manipulation of Δtau with PPARγ agonist/antagonist, proteasome or calpain inhibitors and the anti-oxidant NAC. ΔTau levels in total extracts of human SK-N-SH neuroblastoma cells (30 μg of protein/lane) were assessed by western blot analysis with the Tau C3 antibody (tau cleaved at Asp421, epitope a.a. 412–421). Cells were treated for 16 h with DMSO (vehicle, control, *lanes 1a and 1b*) or with 20 μM PGJ2 alone (*lanes 2a and 2b, boxed*) or with 20 μM PGJ2 after a 40-min pre-incubation with BADGE (*lane 3a*, PPARγ antagonist), pan caspase inhibitor (Z-VAD-FMK, *lane 4a*), or NAC (*lane 6b, boxed*, anti-oxidant). Cells were also separately incubated with BADGE (*lane 5a*), pan caspase inhibitor (*lane 6a*), ciglitazone (PPARγ agonist, *lane 7a*), proteasome inhibitor (*lanes 4b and 5b*), calpain inhibitor (*lane 3b*), or NAC (*lane 7b*). The levels of Δtau, cleaved PARP and actin were semi-quantified by densitometry. The data represent the ratio of Δtau/actin (*black bars*) and ΔPARP/actin (white bars) for all conditions compared to the PGJ2-treatment by itself, which was considered to be 100%. Similar results were obtained in duplicate experiments. Molecular mass markers in kDa are shown on the right. ΔTau, tau cleaved at Asp421; ⋆, unspecific band.

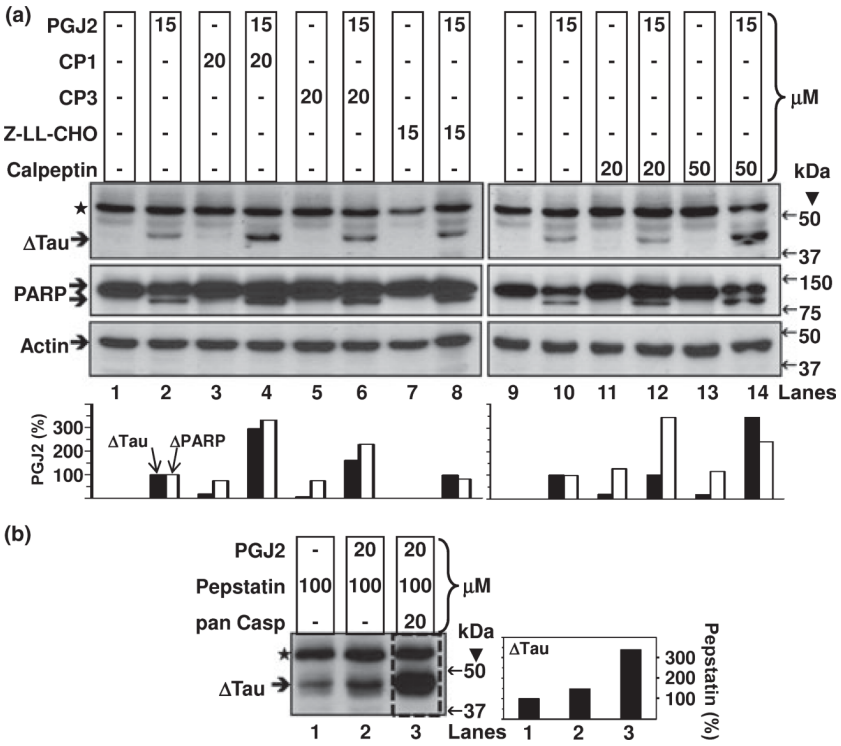


**Fig. 6.**

Calpain inhibitors fail to attenuate the PGJ2-dependent increase in Δtau levels while cathepsin inhibition stabilizes Δtau. ΔTau levels in total extracts of human SK-N-SH neuroblastoma cells (40 μg of protein/lane) were assessed by western blot analysis with the Tau C3 antibody (tau cleaved at Asp421, epitope a.a. 412–421). Cells were treated for 16 h with DMSO (*vehicle, control, lanes 1a and 9a*) or with 15 μM PGJ2 alone (*lanes 2 a and 10a*) or with 15 μM PGJ2 after a 40-min pre-incubation with calpain inhibitors (CP1, *lane 4a*, CP3, *lane 6a*, Z-LL-CHO, *lane 8a*, and calpeptin, *lanes 12a and 14a*). Cells were also treated for 16 h with 20 μM PGJ2 after a 40-min pre-incubation with a cathepsin inhibitor alone (pepstatin, *lane 2b*) or in combination with the pan caspase inhibitor (pan casp, *lane 3b*). Cells were also separately incubated with the calpain inhibitors or pepstatin (*lanes 3a, 5a, 7a, 11a, 13a and 1b*). The levels of Δtau, cleaved PARP and actin were semi-quantified by densitometry. In (a), the data represent the ratio of Δtau/actin (*black bars*) and ΔPARP/actin (*white bars*) for all conditions compared to the PGJ2-treatment by itself, which were considered to be 100%. In (b), the data represent the ratio of Δtau/⋆ for all conditions compared to the pepstatin-treatment by itself, which we considered to be 100%. Similar results were obtained in duplicate experiments. Molecular mass markers in kDa are shown on the right. ΔTAU, tau cleaved at Asp421; ⋆, unspecific band.

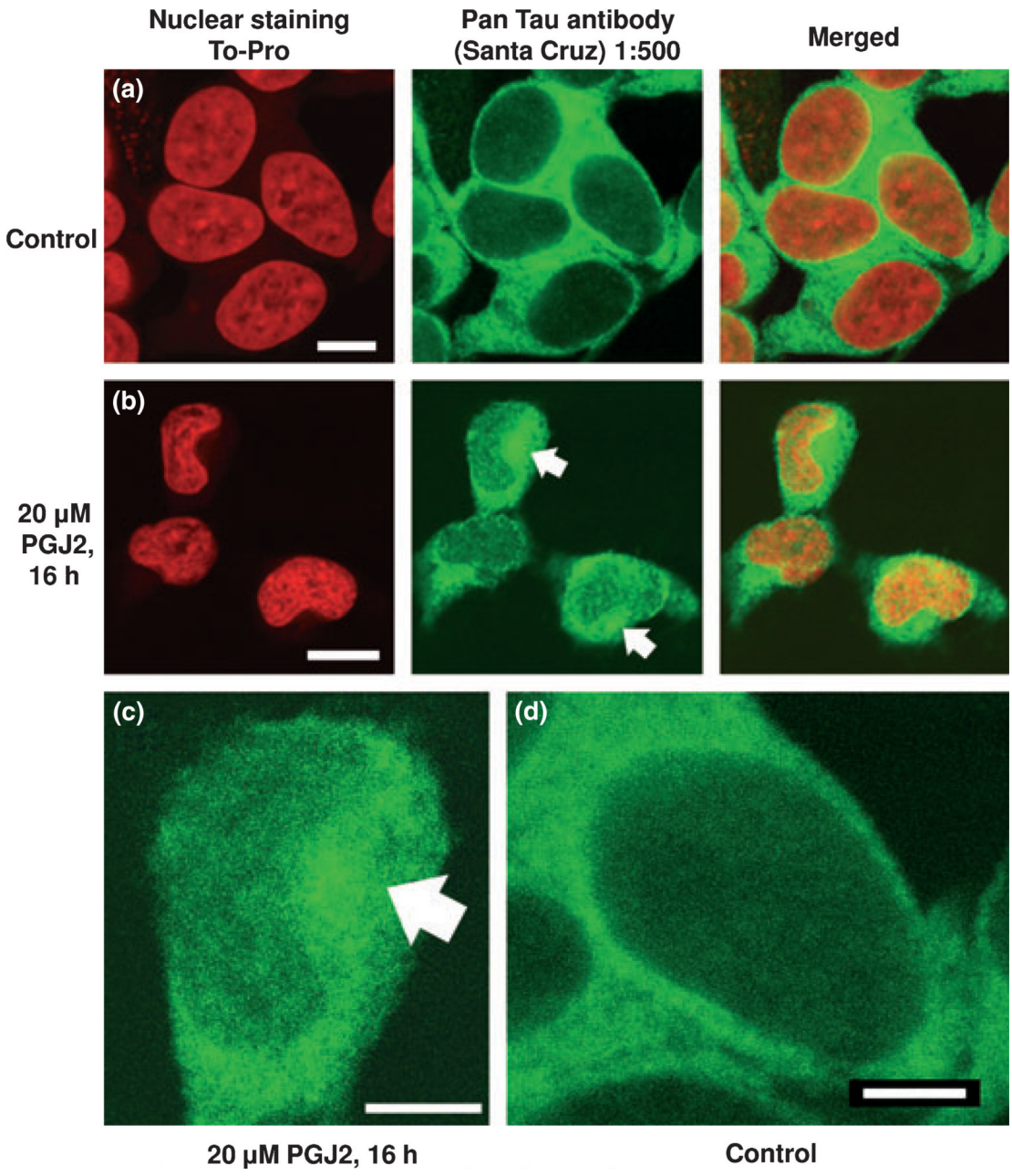


**Fig. 7.**

PGJ2-treatment triggers the formation of tau aggregates. Immunofluorescence staining of SK-N-SH cells treated with vehicle only (DMSO, *a and d*)or 20 μM PGJ2 (*b and c*) for 16 h. Tau (*green*) was visualized by immunostaining with the pan tau antibody (Santa Cruz). Nuclei (*red*) were detected with TO-PRO-3. Merged images are shown for tau/To-Pro. *Arrows* point to large tau aggregates. The scale bar is 7.3 μm (a), 11.9 μm (b), 5.5 μm (c) and 3.6 μm (d). Similar results were obtained in duplicate experiments.

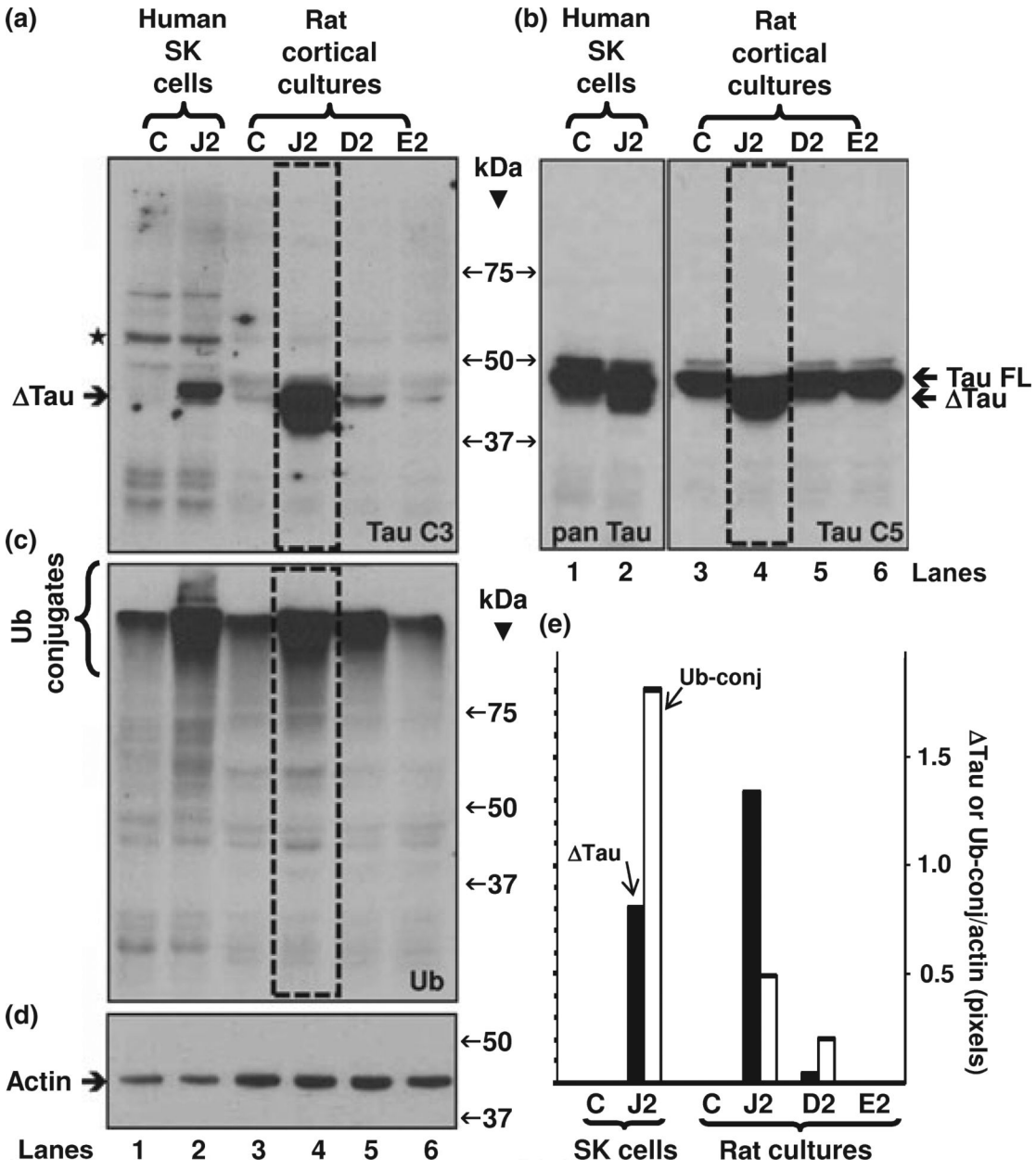


**Fig. 8.**

PGJ2-treatment and to a lesser extent PGD2, induce tau cleavage at Asp421 and accumulation of ubiquitinated proteins in rat (E18) primary cortical neuronal cultures, but PGE2 does not. Western blot analyses (45 μg of protein/lane) to detect tau in total extracts of rat primary cortical cultures treated with DMSO (vehicle, control, C), 20 μM PGJ2 (J2), 20 μM PGD2 (D2) or 80 μM PGE2 (E2) and in SK-N-SH cells (positive control) treated with DMSO (vehicle, control, C) or 20 μM PGJ2 (J2) for 16 h. The blot was probed with the TauC3 antibody (a) then stripped and reprobed with the pan tau clone 5 antibody for the rat cultures or the pan tau clone 13 antibody for the SK-N-SH cells (b). The blot was stripped and reprobed again with the anti-ubiquitinated (Ub) proteins antibody (c). Equal protein loading (6 μg of protein/lane) was demonstrated by probing parallel immunoblots with the anti-actin antibody (d). The levels of Δtau, ubiquitinated proteins (*Ub-conj*) and actin were semi-quantified by densitometry (e). The data represent the pixel ratio of Δtau/actin (*black bars*) and Ub-conj/ actin (white bars) for all

conditions. The values obtained under control (no PGJ2) conditions were subtracted from each sample. Similar results were obtained in duplicate experiments. Molecular mass markers in kDa are shown in the middle. ΔTau, tau cleaved at Asp421; TAU FL, full length tau; ⋆, unspecific band.

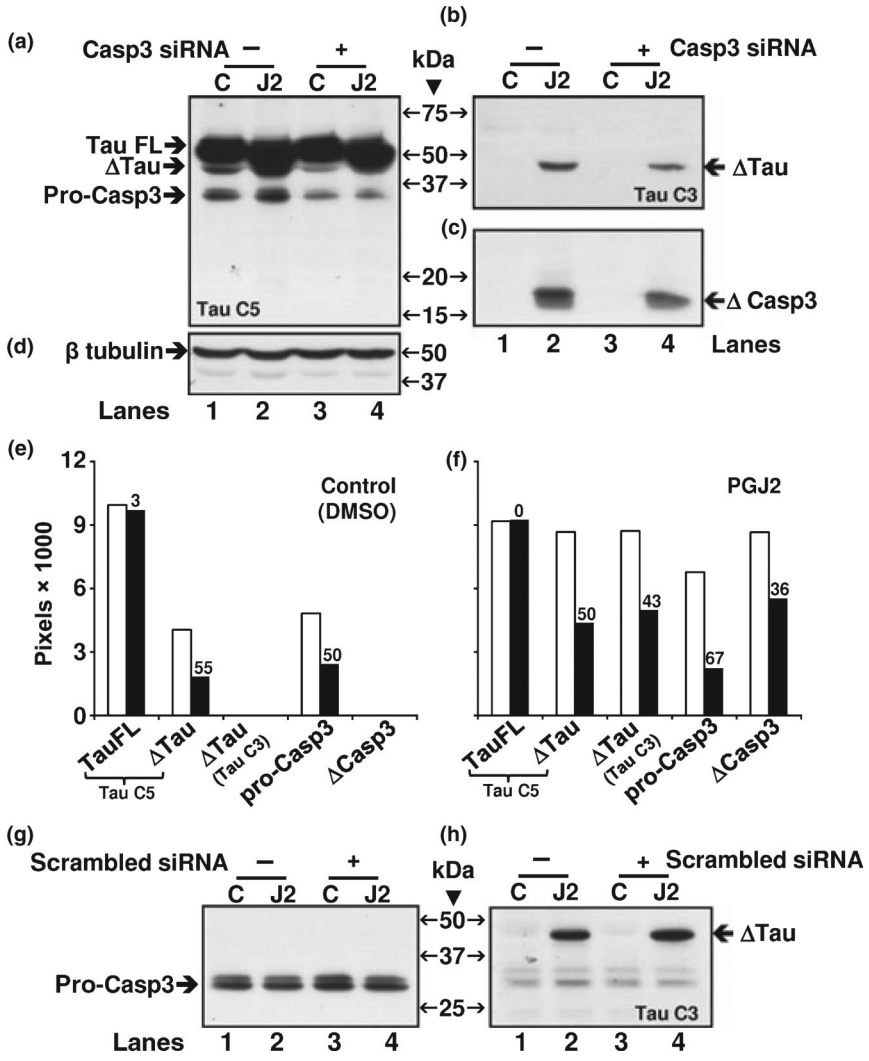


**Fig. 9.**

Caspase 3 knockdown by siRNA decreases the levels of PGJ2-induced tau cleavage at Asp421 in rat (E18) primary cortical neuronal cultures. Neuronal cultures were treated with Caspase 3 (Casp3) siRNA at 80 nM and total lysates were analyzed by western blotting (18 μg of protein/lane) to detect in (a) full length (FL) and cleaved (Δ) tau as well as pro-caspase 3, in (b) Δtau, in (c) cleaved (Δ) caspase 3 and in (d) β tubulin, as loading control. Following siRNA incubations (6 h) the cortical cultures were treated with DMSO (vehicle, control, C) or 20 μM PGJ2 (J2) for 16 h. The same blot was probed sequentially with the TauC3, caspase 3, pan TauC5 and β tubulin antibodies. The levels of tauFL, Δtau, pro-caspase3 (*pro-Casp3*) and cleaved caspase3 (Δ*Casp3*) were semi-quantified by densitometry (e and f). The graphs correspond to control (e) and PGJ2-treated (f) cultures. Within each graph, the *white bars* represent untreated cultures (*no Casp3 siRNA*) and *black bars* represent cultures treated with Casp3 siRNA. The numbers above the *black bars* correspond to the percent decrease in expression because of the Casp3 siRNA treatment. As a control, cells were treated with a scrambled siRNA instead of the Casp 3 siRNA and probed for Δtau (h) and procaspase 3 (g). Molecular mass markers in kDa are shown in the middle. ΔTAU, tau cleaved at Asp421; TAU FL, full length tau.

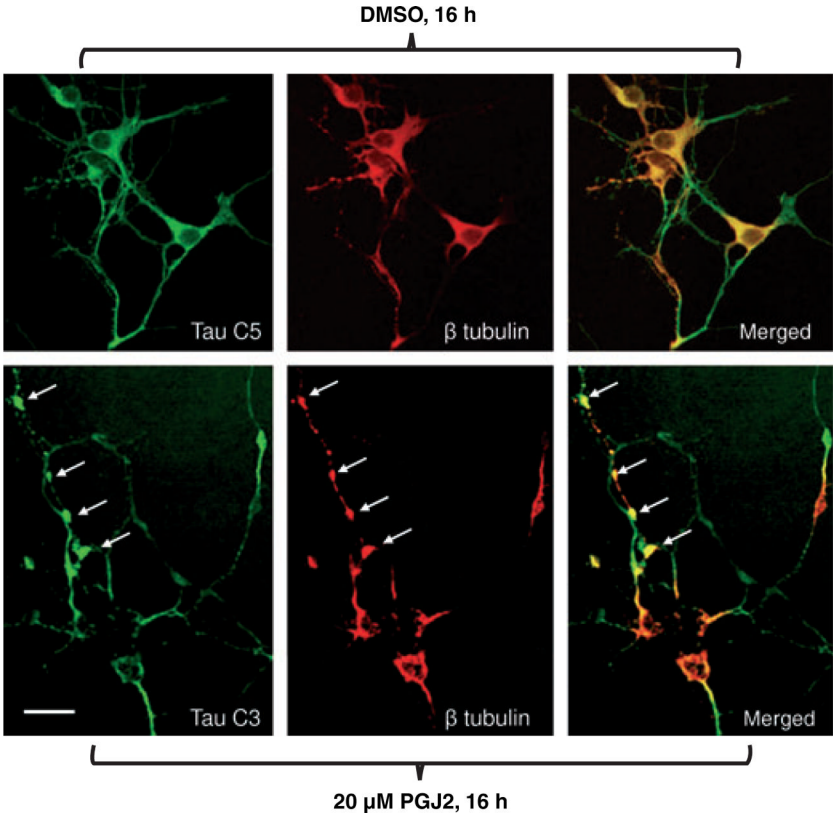


**Fig. 10.**

PGJ2 induces neurite dystrophy in rat (E18) primary cortical neuronal cultures. TAU (*green*) and β tubulin (*red*) immunofluorescent staining of rat cortical neurons treated with DMSO (*top panels*)or 20 μM PGJ2 (*bottom panels*) for 16 h. ΔTau was detected in the PGJ2-treated cells with the TauC3 antibody (*lower panel*). In control cells (*upper panels*) tau was detected with the TauC5 antibody as no immunofluorescence was detected with the TauC3 antibody, which is specific for Δtau. The *arrows* are pointing to dystrophic neuritis. Scale bar = 15 μm. Similar results were obtained in duplicate experiments.

## Table 1

Antibody reactivity. Amino acid (a.a.) numbers correspond to residues on the longest tau isoform, i.e. human tau 40 with 441 residues

| Antibody | Antigen |
|---|---|
| Tau C3 mouse monoclonal | Δtau (ep: a.a. 412–421). Also detects an unspecific band (MW ~60 kDa) in SK-N-SH cells but not in rat primary cortical cultures |
| Tau C5 mouse monoclonal | All tau isoforms and Δtau (ep: a.a. 210–241) |
| Tau 13 (pan tau) mouse monoclonal | All tau isoforms of human origin and Δtau (ep: a.a. 2–18) |
| Tau Y9 rabbit polyclonal | All tau isoforms (ep: a.a. 12–27) |
| β-tubulin rabbit monoclonal | β-tubulin |
| Ubiquitin rabbit polyclonal | Higher affinity for polyubiquitin conjugates than for monoubiquitin |
| PARP mouse monoclonal | Full length and cleaved PARP |
| Caspase 3 rabbit polyclonal | Full length and cleaved caspase 3 |
| Actin mouse monoclonal | Actin |

Δtau, tau cleaved at Asp 421; ep, epitope; PARP, poly (ADP-ribose) polymerase.